Published in final edited form as:
J Am Chem Soc. 2012 September 19; 134(37): 15245–15248. doi:10.1021/ja3066896.

Analysis of DNA-Guided Self Assembly of Microspheres Using Imaging Flow Cytometry

Hao Tang[†], **Ryan Deschner**[†], **Peter Allen**[‡,#], **Younjin Cho**[‡,§], **Patrick Sermas**[†], **Alejandro Maurer**[†], **Andrew D. Ellington**[‡,#], and **C. Grant Willson**[*,†,‡]

[†]Department of Chemical Engineering, The University of Texas at Austin, Austin, TX 78712, United States

[‡]Department of Chemistry and Biochemistry, The University of Texas at Austin, Austin, TX 78712, United States

[#]Institute for Cellular and Molecular Biology, The University of Texas at Austin, Austin, TX 78712, United States

Abstract

Imaging flow cytometry was used to analyze the self assembly of DNA-conjugated polystyrene microspheres. This technique enables quantitative analysis of the assembly process and thereby enables detailed analysis of effect of structural and process variables on the yield of assembly. In a demonstration of the potential of this technique, the influence of DNA strands base pair (bp) length was examined and it was found that 50 bp was sufficient to efficiently drive the assembly of microspheres, forming not only dimers but also chain-like structures. The effect of stoichiometry on yield was also examined. The analysis demonstrated that self assembly of 50 bp microspheres can be driven to near completion by stoichiometric excess in a manner similar to Le Chatelier's principle in common chemical equilibrium.

Keywords

Self Assembly; DNA; Flow Cytometry

DNA-directed self-assembly has attracted both scientific and technological interest. The use of DNA as a "smart glue" in self-assembly imparts many advantages, including high specificity[1], thermal reversibility[2], and modulation of assembly by factors such as nucleases[3], competitive displacement[4], or photocrosslinking[5]. These advances are beginning to herald applications in a variety of fields, spanning from disease diagnosis[6] to nanoelectronics[7,8]. Most intriguingly, studies of DNA-mediated colloidal crystallization[9-11] have shown that there may be an intimate relationship between building block properties and lattice parameters of the resultant self-assembled solids.

Unfortunately, it is often difficult to fully characterize the morphologies and the distribution of morphologies that are created by DNA-directed assembly of particles, much less couple the characteristics of individual particles to the yield and characteristics of larger aggregates.

[*]Corresponding Author: Telephone: 512-471-4342. Fax: 512-471-7222. willson@che.utexas.edu.
[§]Current address: Semiconductor Materials R&D Center, Cheil Industries Inc., Samsung, 332-2 Gocheon-Dong, Uiwang-Si, Gyeonggi-Do, 437-711, Korea

ASSOCIATED CONTENT

Supporting Information. Experimental procedures for the DNA conjugation, flow cytometry methods, additional cytometry charts, and fluorescence microscopy images. This material is available free of charge via the Internet at http://pubs.acs.org.

Many methods have been used to characterize and follow the progress of self-assembly, including UV-visible spectroscopy[9,12], optical and fluorescence microscopy[2-4], electron microscopy[9,11-13], light scattering[12,13], and X-ray diffraction[10,11]. However these tools are largely used to characterize bulk properties, rather than study individual particles in what are generally complex mixtures and distributions of assembly products and aggregates.

In this regard, flow cytometry[14] is particularly well-suited to analyze the self-assembled clusters of micronsized particles. Flow cytometry is a cell-biology technique that rapidly measures the optical properties of individual cells. It gives statistically robust, quantitative counting results by measuring the scattering and/or fluorescence intensity from thousands of suspended particles as they pass one-by-one through an optical detector region. C. Soto et al.[15] have previously used flow cytometry to estimate the assembly yield of submicron polystyrene particles. Recently, imaging flow cytometry[16-18], a technique combining conventional flow cytometry with high-speed microscopy, has become available. Traditional cytometry gives intensity values for each particle as a function of wavelength, but imaging flow cytometry provides these data together with a fluorescence micrograph of each particle. Therefore, imaging flow cytometry analysis of DNA-guided microsphere assembly generates a detailed report describing both the number and morphology of different types of assemblies. These data enable an analysis of the details of the assembly distribution as a function of changes in the substrate, DNA sequence, reaction conditions, etc. that provide guidance for production of useful, large scale assemblies.

The DNA-conjugated particles in this study were prepared via coupling of carboxylate-modified polystyrene (PS) microspheres and amine-modified DNAs using 1-ethyl-3-(3-dimethylamino-propyl) carbodiimide (EDC). The DNA strands A and B (A' and B', A" and B") are fully complementary, and their sequences are listed in Table 1. Fluorescent dyes were used to label and follow the DNAs or PS microspheres. Figure 1 depicts the construction of PS beads and their subsequent assembly in which the polyvalent presentation of DNA on the PS microspheres generates a distribution of assemblies, including dimers, trimers, and higher order aggregates.

Dual-color fluorescent labeling was employed so that different self-assembled microsphere aggregates can be readily distinguished. Figure 2 shows a double fluorescence scatter plot and fluorescent micrographs for an experiment in which 6μm-diameter PS beads conjugated with the complementary DNA strands A and B were assembled. In the double fluorescence scatter plot, the fluorescence intensities at two different wavelengths are plotted against each other for each particle cluster. For example, the unbound A beads (blue color) reside near the x-axis because they have a high Cy3 fluorescence intensity but almost zero Cy 5 intensity. Likewise, the B beads (yellow color) reside near the y-axis, and the A-B assemblies reside in the middle of the plot. The A-B assemblies can be further resolved into distinct sub-populations, including dimers (AB), trimers (A_2B and AB_2), and tetramers (A_2B_2). The validity of assignment within the plot was confirmed by studying the fluorescence micrographs in Figure 2(b). The yield of each type of aggregate was established in this manner. In this experiment the assembly produced mainly dimers, with few trimer and tetramer assemblies (171 AB, 6.7%; 12 A_2B, 0.5%; 21 AB_2, 0.8%; - A_2B_2, 0.2 %). We also notice a significant number of homodimers (126 AA, 4.9% and 179 BB, 7.0%), which may result from the formation of secondary structures (Supporting Figure S1, Table S1).

It has been reported that DNA complementarity as short as 12bp is adequate to drive the assembly of 1μm and 2μm beads[19]. While 18bp fully-complementary A and B strands can drive the assembly of 6μm beads in a static fluorescence microscopy setup (Figure S2), the 18bp complement provides only a low assembly yield in flow cytometry. The majority of

the assembly products fail to survive the shearing force in the flow environment. These data provide important input to those who are designing large macroscopic structures that are to be generated by DNA-mediated self assembly.

Imaging flow cytometry was used to investigate the effect of DNA length and melting point on assembly yield; these data are summarized in Table 2. The melting point of the 25bp DNA pair, A'-B' is 17 degrees higher than that of the 18bp A-B pair. Increasing the melting point increased the assembly yield from 8.4% to 59.5% (Figure S3). Interestingly, the 50bp poly-adenosine and poly-thymidine DNA pairing, A"-B", which has a melting point very close to that of A'-B', gave a nearly identical assembly yield (58.8%). The DNA melting point seems to be an important factor that should be considered in the design of DNA-guided self-assembly of microspheres.

As shown in Figure 3, the population of dimer pairs of the 50 bp microsphere, A"-B" beads (58.8%) is more than twice that of the unbound population of A" and B" beads (21.3% and 19.9%, respectively). Some higher order assemblies are observed including chains with length ≥7 beads. Through examination of the fluorescent micrographs, flow cytometry enables verification that these chains have a precise, alternating arrangement of the two beads as can be seen in Figure 3b. It is important to report that as expected, mixture of beads with non-complementary sequences show very little binding to one another (Table 2, Figure S5). The fact that the majority of the high order assemblies generated in these experiments are chain like rather than spherical morphologies may be the result of the shear fields generated in the flow channels of the imaging flow cytometer[21].

The stoichiometric ratio of *A to* B beads was controlled to be 1:1 in the experiments above. We found that an excess of A (or B) can drive the assembly to near completion in a manner similar to Le Chatelier's principle. Figure 4 shows the change in assembly populations that occurs when different ratios of 6μm A" and B" beads were mixed. At an A"/B" ratio of 0.6, the incorporation of B" into assemblies was 54.9%, while at an A"/B" ratio of 9.6, the incorporation of B" increased to 98.1% (Table S2). Increasing the A"/B" ratio also has a profound effect on the structure of the assembly. When the A"/B" ratio is close to 1, the major population of assembly is A"B"$_n$ (Figure 4a, b). As the A"/B" ratio increases, the population of A"$_2$B"$_n$ and A"$_3$B"$_n$ exceeds A"B"$_n$ (Figure 4c) and finally predominates (Figure 4d, e).

The imaging flow cytometer was also used study to the effect variations in the assembly of structures created by mixing beads of different sizes. As shown in Figure 5, when 6μm A" beads were mixed with 3μm B" beads in a ration of 1:10, a different aggregate structure forms, with A" beads binding to multiple B" beads. The average coordination number of A" beads bound to B" beads was 3.2. In contrast, when 6μm A" and 6μm B" beads were assembled in 1:1 ratio (Figure 3), the average coordination number was 1.0, but when they were assembled in 9.6:1 ratio (Figure 4), the average coordination number was 2.3. The high coordination number in Figure 5 is the result of both heterogeneous bead size and stoichiometric excess.

The increased coordination number suggests that DNA-guided self assembly systems tend to maximize the total number of DNA hybridization events, which is consistent with the guidelines proposed by C. Mirkin et al. in nanoscale DNA-guided crystallization[11]. Nevertheless, self assembly at the mesoscale (micron level) engenders more challenges. Both gravity and flow-induced kinetic energy increase as the third power of particle size, while the DNA hybridization energy scales with surface area, i.e., the second power of particle size. Therefore, mesoscale DNA-guided self assembly requires stronger DNA hybridization interactions.

DNA-guided crystallization can enable new technologies such as self assembled photonic crystals. In addition, the ability to synthesize and characterize library of particles with faces that are substituted with varying DNA sequences provides access to another broad spectrum of applications. For example, the porous nature of a microsphere assembly provides a path to creation of new low-k dielectric materials for microelectronics[22]. Self-assembled amorphous materials are also receiving a great deal of attention as battery electrodes[23] and hydrogen storage materials[24]. Although the DNA-coated PS microspheres described in this study are isotropic and as such, do not yet impart orientational control, the recent advances in Janus particle fabrication[25,26] promise control of more complex mesoscale particle assemblies in the near future. The rate of progress toward that end can be significantly increased through use of imaging flow cytometry as an analytical tool.

Supplementary Material

Refer to Web version on PubMed Central for supplementary material.

Acknowledgments

The authors thank the UT Genome Sequencing and Analysis Facility for the equipment support, as well as Dr. Xi Chen and Dr. Aleksandr Miklos for fruitful discussions. This work was supported by the Rashid Engineering Reagents Chair, National Security Science and Engineering Faculty Fellowship (FA9550-10-1-0169), National Institute of Health (1 R01 GM094933-01) and the Welch Foundation (F-1654) and the Virginia and Ernest Cockrell, Jr. Fellowship in Engineering.

REFERENCES

(1). Rothemund PW. Nature. 2006; 440:297. [PubMed: 16541064]

(2). Valignat MP, Theodoly O, Crocker JC, Russel WB, Chaikin PM. Proceedings of the National Academy of Sciences of the United States of America. 2005; 102:4225. [PubMed: 15758072]

(3). Tison CK, Milam VT. Biomacromolecules. 2008; 9:2468. [PubMed: 18715032]

(4). Tison CK, Milam VT. Langmuir : the ACS journal of surfaces and colloids. 2007; 23:9728. [PubMed: 17696456]

(5). Rajendran A, Endo M, Katsuda Y, Hidaka K, Sugiyama H. Journal of the American Chemical Society. 2011; 133:14488. [PubMed: 21859143]

(6). Storhoff JJ, Elghanian R, Mucic RC, Mirkin CA, Letsinger RL. Journal of the American Chemical Society. 1998; 120:1959.

(7). Keren K, Berman RS, Buchstab E, Sivan U, Braun E. Science. 2003; 302:1380. [PubMed: 14631035]

(8). Maune HT, Han S.4p. Barish RD, Bockrath M, Goddard IIA, RothemundPaul WK, Winfree E. Nature nanotechnology. 2010; 5:61.

(9). Mirkin CA, Letsinger RL, Mucic RC, Storhoff JJ. Nature. 1996; 382:607. [PubMed: 8757129]

(10). Nykypanchuk D, Maye MM, van der Lelie D, Gang O. Nature. 2008; 451:549. [PubMed: 18235496]

(11). Macfarlane RJ, Lee B, Jones MR, Harris N, Schatz GC, Mirkin CA. Science. 2011; 334:204. [PubMed: 21998382]

(12). Maye MM, Nykypanchuk D, Cuisinier M, van der Lelie D, Gang O. Nature materials. 2009; 8:388.

(13). Tikhomirov G, Hoogland S, Lee PE, Fischer A, Sargent EH, Kelley SO. Nature nanotechnology. 2011; 6:485.

(14). Shapiro, HM. Practical Flow Cytometry. John Wiley & Sons; 2003.

(15). Soto CM, Srinivasan A, Ratna BR. Journal of the American Chemical Society. 2002; 124:8508. [PubMed: 12121074]

(16). Bonetta L. Nat Meth. 2005; 2:785.

(17). Basiji DA, Ortyn WE, Liang L, Venkatachalam V, Morrissey P. Clinics in Laboratory Medicine. 2007; 27:653. [PubMed: 17658411]

(18). Helguera G, Rodríguez JA, Luria4Pérez R, Henery S, Catterton P, Bregni C, George TC, MartínezMaza O, Penichet ML. Journal of Immunological Methods. 2011; 368:54. [PubMed: 21420412]

(19). Milam VT, Hiddessen AL, Crocker JC, Graves DJ, Hammer DA. Langmuir : the ACS journal of surfaces and colloids. 2003; 19:10317.

(20). Zadeh JN, Steenberg CD, Bois JS, Wolfe BR, Pierce MB, Khan AR, Dirks RM, Pierce NA. Journal of Computational Chemistry. 2011; 32:170. [PubMed: 20645303]

(21). Rabideau BD, Bonnecaze RT. Langmuir : the ACS journal of surfaces and colloids. 2007; 23:10000. [PubMed: 17711312]

(22). Volksen W, Miller RD, Dubois G. Chemical Reviews. 2009; 110:56. [PubMed: 19961181]

(23). Wang H, Wu Y, Bai Y, Zhou W, An Y, Li J, Guo L. Journal of Materials Chemistry. 2011; 21:10189.

(24). Jeon YM, Armatas GS, Heo J, Kanatzidis MG, Mirkin CA. Advanced Materials. 2008; 20:2105.

(25). Jiang S, Chen Q, Tripathy M, Luijten E, Schweizer KS, Granick S. Advanced Materials. 2010; 22:1060. [PubMed: 20401930]

(26). Nie Z, Li W, Seo M, Xu S, Kumacheva E. Journal of the American Chemical Society. 2006; 128:9408. [PubMed: 16848476]

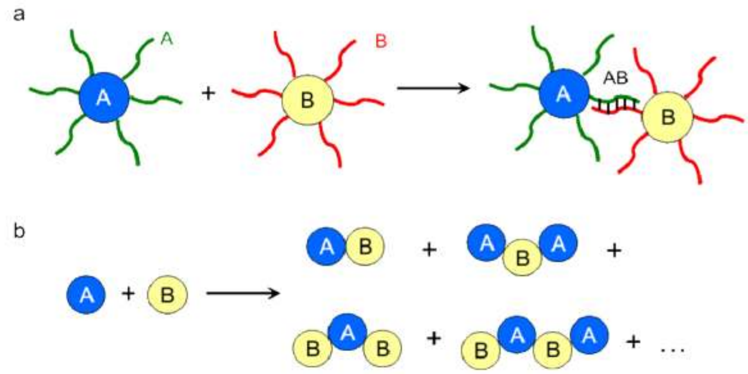

Figure 1.

Assembly scheme of polyvalent polystyrene (PS) microspheres using DNA. (a) Complementary DNA strands (A and B) were conjugated onto PS microspheres. (b) The polyvalent nature of these PS microspheres yields a mixture of aggregates, including dimer (AB), trimer (A_2B and AB_2), tetramer (A_2B_2), etc. DNA strands were omitted for clarity.

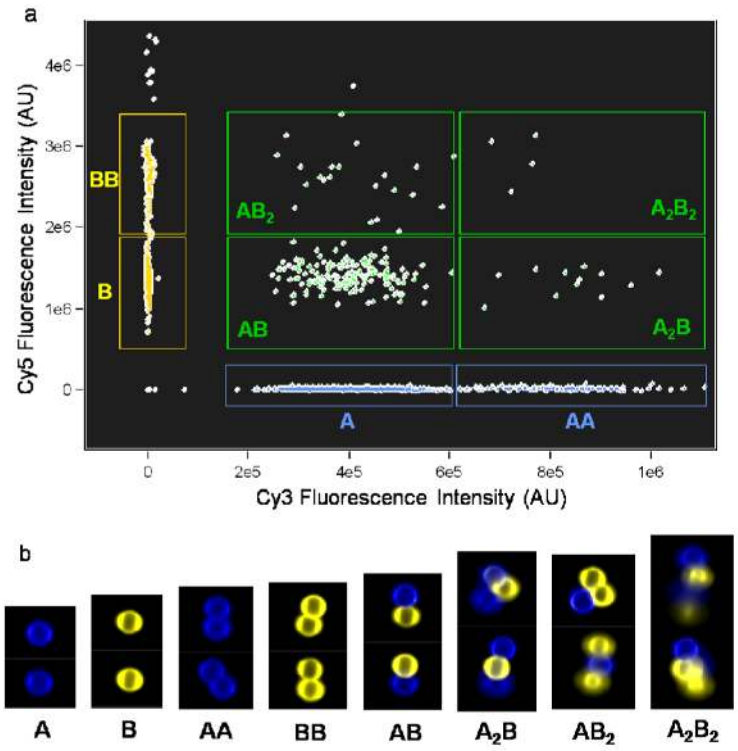

Figure 2.

(a) Imaging flow cytometry chart of 6μm-diameter PS beads assembly. The beads were conjugated with DNA strands A (Cy3 fluorophore, blue color) and B (Cy5 fluorophore, yellow color). The fluorescence intensities have been compensated to remove the coupling due to spectral overlap and free DNA hybridization (Figure S4). (b) Representative fluorescent micrographs of beads in each assigned region.

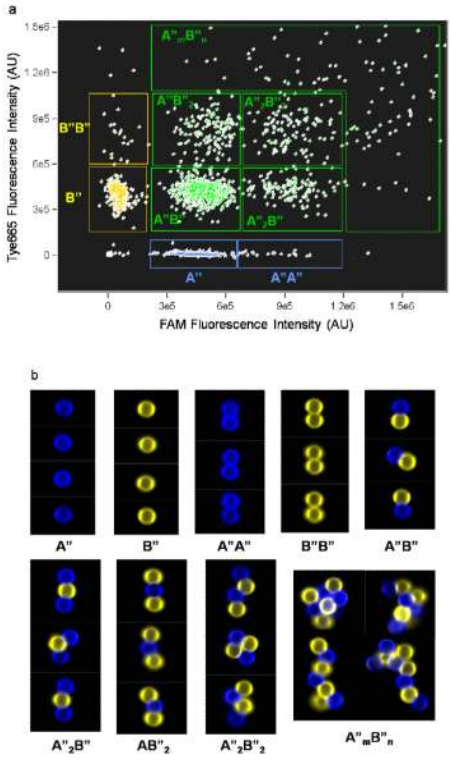

Figure 3.

(a) Imaging flow cytometry chart of 6μm-diameter PS beads assembly. The DNA strands were A“ (FAM fluorophore, blue color) and B” (Tye 665 fluorophore, yellow color). The A“$_m$B”$_n$ region extends beyond the upright corner, and only part of the region is shown here for clarity. (b)

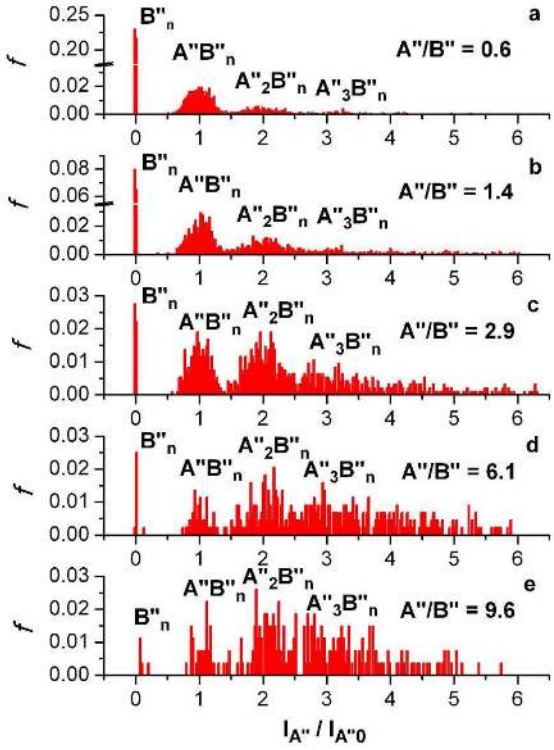

Figure 4.

FAM fluorescence intensity histogram of assembly products from 6μm A“ and 6μm B” beads. (a) A“/B”=0.6, (b) A“/B”=1.4, (c) A“/B”=2.9, (d) A“/B”=6.1, (e) A“/B”=9.6. *f*: relative frequency. $I_{A“}$: FAM fluorescence intensity. $I_{A”0}$: average FAM fluorescence intensity of A“ monomer. The ratio $I_{A”}/I_{A“0}$ roughly indicates the number of A” bead in a certain bead assembly.

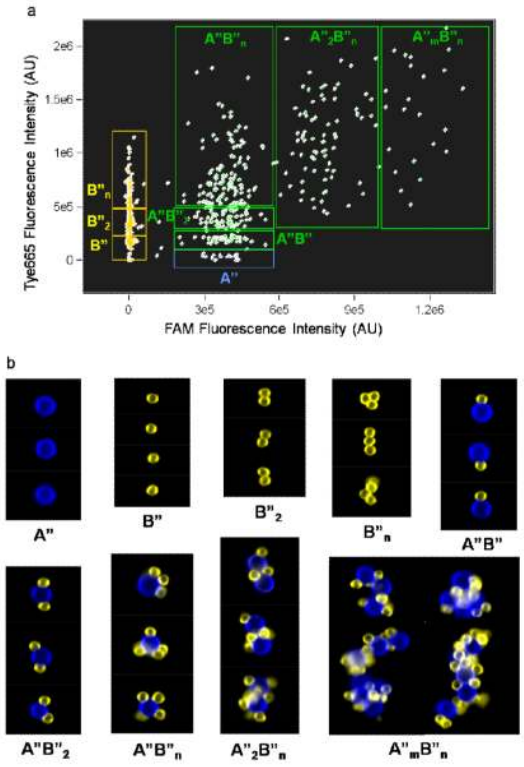

Figure 5.

(a) Imaging flow cytometry chart of 6μm-diameter A“ beads and 3μm B” beads. The ratio of B“ beads to A” beads is 10:1. The A“$_m$B”$_n$ region extends beyond the upright corner, and only part of the region is shown here for clarity. (b) Representative fluorescent micrographs of beads in each assigned region.

Table 1

DNA Sequences (5′→3′)[a]

Name	Sequence
A	/5AmMC6/ ATACG CACAT GCCTG TTT /3Cy3Sp/
B	/5AmMC6/ AAACA GGCAT GTGCG TAT /3Cy5Sp/
A’	/5AmMC6/ TATGC GTATG TATGC GTGCG TGCGT[b]
B’	/5AmMC6/ ACGCA CGCAC GCATA CATAC GCATA
A”	/56FAM/ (AAAAA AAAAA)5 /3AmMO/
B”	/5TYE665/ (TTTTT TTTTT)5 /3AmMO/
C	/56FAM/ TACAT GCAGT GCGTC TTT /3AmMO/[c]

[a]The functional groups and fluorescent labels are written in the sequence format of Integrated DNA Technologies. /5AmMC6/: 5′ end amine modifier with C6 linker; /3Cy3Sp/: 3′ end Cy3 label; /3Cy5Sp/: 3′ end Cy5 label; /56FAM/: 5′ end 6-FAM label; /3AmMO/: 3′ end amine modifier; /5TYE665/: 5′ end TYE 665 label.

[b]DNA A’ and B’ do not have fluorescent labels. Instead, fluorescent dye fluorescein cadaverine or texas red cadaverine was conjugated to the unreacted carboxylic acid groups on the PS microspheres after DNA conjugation.

[c]Strand C is a mismatch sequence as a negative control.

Table 2

DNA Length and Assembly Yield[a]

Sequence	Length (bp)	mp (°C)[b]	Yield (%)[c]
A+B	18+18	41	8.4
A'+B'	25+25	58	59.5
A"+B"	50+50	56	58.8
B"+C	50+18	NA	0.7

[a]The diameter of microspheres was 6μm and their stoichiometry was 1:1.

[b]DNA melting point was calculated using NUPACK online server[20] at 10pM DNA concentration and 0.1M Na^+ concentration.

[c]Yield is defined as number of A-B assemblies divided by total number of particles. Let A_mB_n denote a bead assembly containing m bead A and n bead B, then yield = (Number of A_mB_n)/(Number of A_mB_n+ Number of A_m+ Number of B_n), where m, n ≥1.